Journal of Computers, Mechanical and Management

Journal homepage: www.jcmm.co.in

Volume 1 Issue 1

Friction Stir Welding of Different Aluminum-Silicon Alloy Compositions Utilizing Conventional Vertical Milling Machine

K. J. Santosh Kumar[a], Ganesh Arjun Bhargav[a], Yuvaraja Naik[b], and K. Bommanna[*c]

[a]Department of Mechanical Engineering, K.S. School of Engineering and Management, Bangalore, Karnataka, India 560109

[b]Department of Mechanical Engineering, Presidency University Bangalore, Karnataka, India, 560064

[c]Department of Mechanical Engineering, A P S College of Engineering, Bangalore, Karnataka, India 560082

Abstract

Friction-Stir Welding (FSW) is a solid-state procedure for welding two plates in which there is relative motion between the tool and workpiece, which creates the heat required for the material of the two edges to join by atomic diffusion. The present research article focuses on friction stir welding of dissimilar aluminum-silicon alloys utilizing a vertical milling machine and altering process parameters. Moreover, testing is done on the weld joints for the best process parameter. The process parameters considered in the present work for joining dissimilar aluminum alloys primarily were a constant tool feed rate of 63 mm/min and three varied tool rotational speed rates of 710, 1000 and 1400 rpm. Mechanical characterization of weld joints, such as tensile, hardness, microstructural studies and surface roughness tests, were used to identify the most optimal parameter. The results indicated that Al-Si alloys having Al-5 %Si with Al-12 %Si FSW joints welded using 1000 rpm tool rotational speed proved to have better hardness and lesser surface roughness while, Al-Si alloys having Al-12 %Si with Al-17 %Si FSW joints, had better hardness and roughness properties when welded using 1400 rpm tool rotational speed. Concerning the ultimate tensile strength, Al-Si alloys having Al-5 %Si with Al-12 %Si and Al-12 %Si with Al-17 %Si FSW joints welded using 1400 rpm tool rotational speed offered better results.

Keywords: Friction Stir Welding; Weld Joints; Aluminum Alloys; Silicon; Mechanical Properties

1 Introduction

Friction-Stir Welding (FSW) is a solid-state procedure for welding two plates in which there is relative motion between the tool and workpiece, which creates the heat required for the material of the two edges to join by atomic diffusion [1] and was developed by The Welding Institute (TWI), in 1991 [2]. TWI successfully obtained patents for FSW in Europe, the United States, Japan and Australia while completing a development study demonstrating FSW as a realistic and viable technology for welding aluminum alloys from the 2XXX, 5XXX, and 6XXX series [3, 4]. Figure 1 depicts a diagrammatic representation of friction stir welding. Unlike traditional fusion welding processes employed for dissimilar materials, the FSW process consumes less time and is cost-effective [5]. Moreover, FSW does not require the melting of material as the temperature involved in this process is significantly lower than the melting temperature of the base materials, and the secondary phase development does not occur during this process [6–10]. Previous studies reveal that of all the process parameters, tool rotational speed and feed rate play a major role in the quality of FSW processed parts [11–13]. The literature reviewed indicated that the wear rate reduces as the tool feed rate increases. However, beyond a certain value, the wear rate begins to increase. The highest resistance to wear was obtained at a tool feed rate of 65 mm/min [6]. The studies also indicated that a tool rotational speed of 1300 rpm showed better quality weld and strength [14].

*Corresponding author: bommannak_cta@rediffmail.com

Received: 13 September 2022; **Accepted:** 29 September 2022; **Published:** 30 October 2022

DOI: 10.57159/gadl.jcmm.1.1.23012.

The present work is unique as it investigates the microstructure, hardness and tensile strength of FSW joints in order to determine the value of process parameters to achieve the best mechanical properties and minimum surface roughness of Al-Si alloy FSW joints, as the investigated properties affect the corrosion behavior, fatigue strength and life cycle of FSW joints.

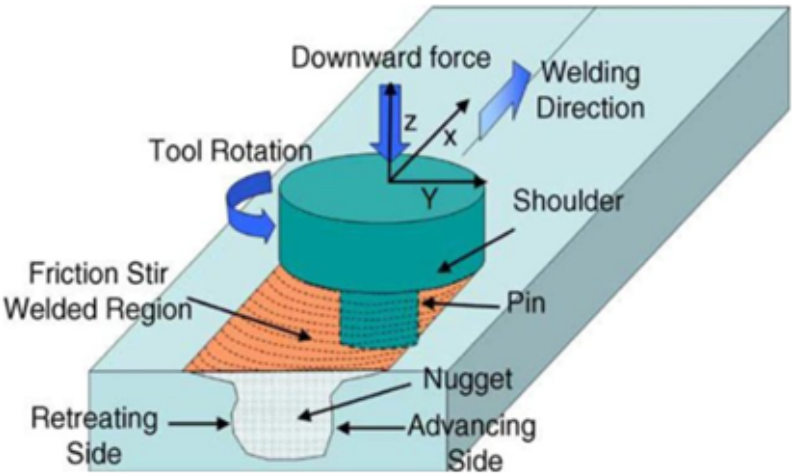

Figure 1: Schematic representation of a friction stir welding process [15].

2 Materials and Method

Conventional milling machines have proved to be used to undertake friction stir welding of aluminum alloys [16]. Therefore, the present work utilizes the laboratory-installed conventional turret mill-based milling machine, as shown in Figure 2(a), for the friction stir welding process. Figure 2(b) depicts an overview of the FSW plate for the shoulder tool-contacting side. This surface was distinguished by the so-called wake effect and the presence of semicircular features similar to those produced by conventional milling [17, 18].

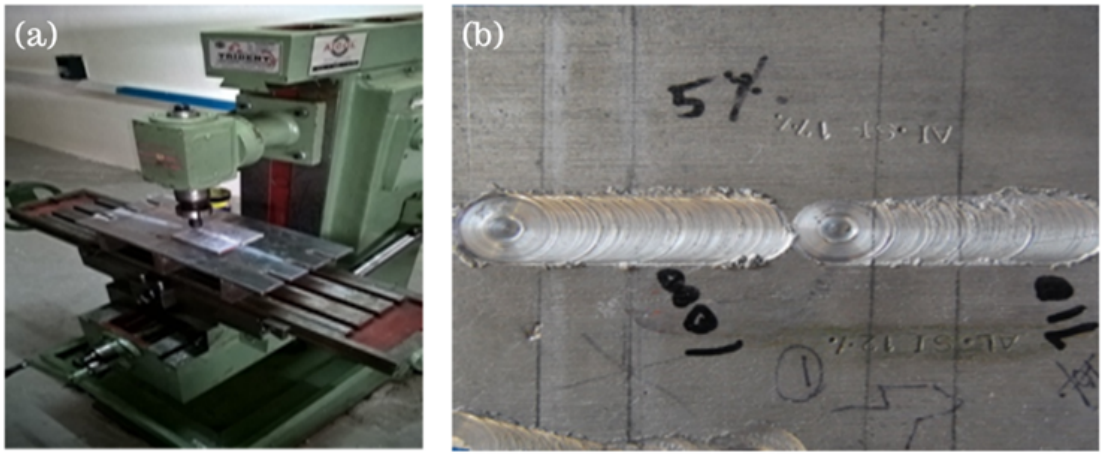

Figure 2: **(a)** Vertical milling machine setup; **(b)** friction-welded Al-Si specimen.

Silicon is the principal alloying ingredient in the Al-Si alloys, as its addition results in good castability and weldability because of its high fluidity and minimal shrinkage properties. Thus, the friction stir welding was performed on two different combinations of three different Al-Si compositions (Al-5 %Si with Al-12 %Si and Al-12 %Si with Al-17 %Si). Tool rotational speed, the most significant process parameter, was varied, and the tool feed rate was maintained constant. The rotational speeds used were 710, 1000 and 1400 rpm, and the feed rate was maintained at 63 mm/min.

2.1 Tensile test

Tensile strength is the ability of a material to withstand fracture when a pulling force is applied. The material with good tensile strength resists higher loads; therefore, it is necessary to check the tensile strength of the joint. The specimens are prepared as per the ASTM standard E08. The dimensions of the tensile test specimens are as shown in Figure 3(a). Tensile test was performed using a universal testing machine, suitable for small loads (less than 2000 kg).

A tensile specimen of Al-Si alloy prepared according to the ASTM standard is shown in Figure 3(b). A few fractured specimens comprising Al-5 %Si with Al-12 %Si and Al-12 %Si with Al-17 %Si FSW joints welded using 710, 1000 and 1400 rpm are shown in Fig. 3(c) from left to right.

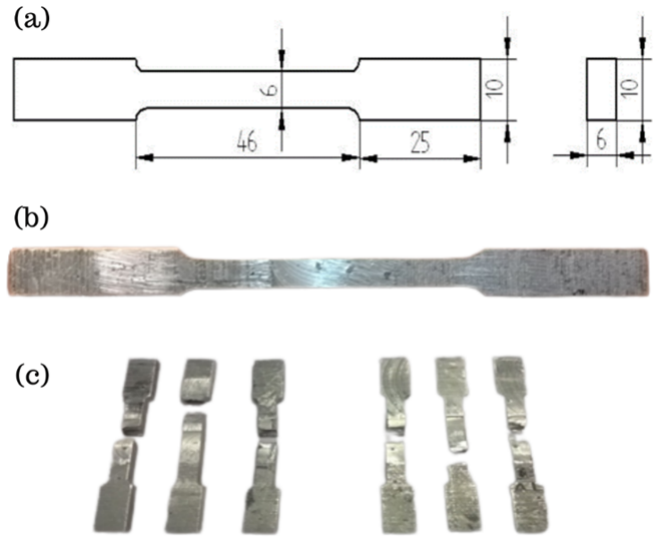

Figure 3: Tensile test specimen: **(a)** standard dimensions used for specimen preparation; **(b)** sample tensile specimen; **(c)** fractured tensile specimen.

2.2 Hardness test

Hardness, a mechanical property of the material, is its resistance to deformation and is assessed by a standard test that measures the material's surface resistance to indentation. It impacts the tribological performance of a material and is also an essential aspect to consider during machining [19]. In simple words, hardness is the property of a material that enables it to resist plastic deformation, penetration, indentation, and scratching. Figure 4(a) shows the laboratory-installed Rockwell hardness testing machine used in the present work, which was used to determine the hardness by comparing the depth of an indenter's penetration under a large force (100 Kgf is the load chosen for the test) to the pre-load penetration.

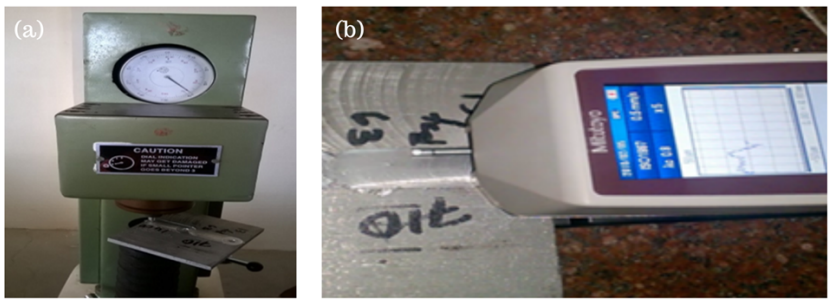

Figure 4: Laboratory equipment used for testing of FSW specimen: **(a)** Rockwell hardness testing machine; **(b)** surface profilometer.

2.3 Surface roughness test

Surface roughness affects working on a surface. Under variable loading conditions, the fracture of welded joints initiates at the component's surface. Consequently, surface roughness has a substantial impact on the fatigue of the welded joint [20]. As depicted in Figure 4(b), a diamond indent stylus profilometer was used to assess the change in longitudinal surface roughness (Ra) caused by the FSW process on the side in contact with the shoulder.

3 Results and Discussion

3.1 Tensile strength

The average experimental values of ultimate tensile strength obtained for Al-5 %Si with Al-12 %Si and Al-12 %Si with Al-17 %Si FSW joints are shown in Table 1. The bar chart in Figure 5 compares the two dissimilar joints at various tool rotational speeds.

Table 1: Ultimate tensile strength of welded joints values of the FSW joints.

Welding condition	Average ultimate tensile strength (MPa)	
	Al-5%Si with Al-12%Si	Al-12%Si with Al-17%Si
710 rpm at 63 mm/min	59.5	88.6
1000 rpm at 63 mm/min	83.0	134.7
1400 rpm at 63 mm/min	89.0	112.7

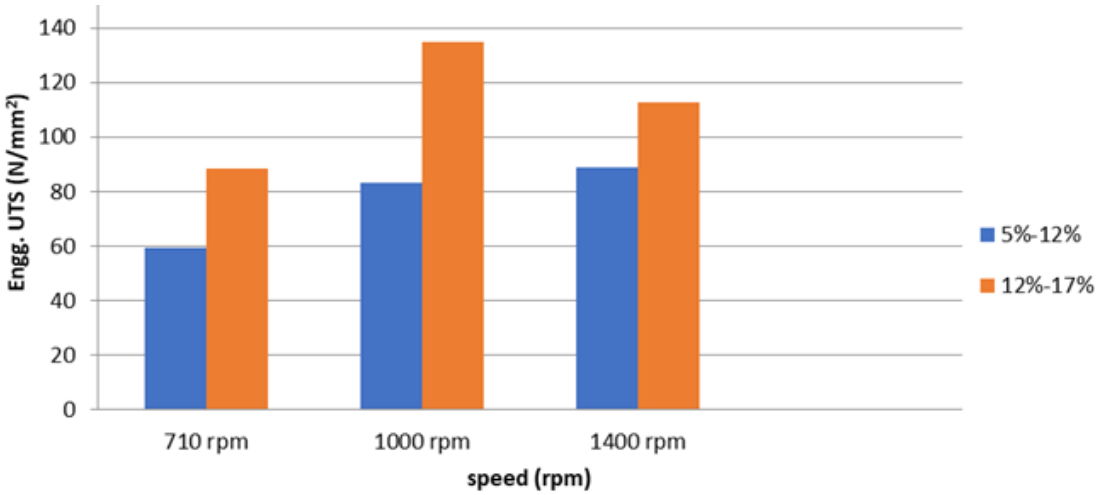

Figure 5: Ultimate tensile strength of various tested FSW joints.

From Figure 5, the comparison between the two dissimilar welded joints at various tool rotational speeds could be observed. The obtained tensile behavior results indicated increased tensile strength with the tool rotational speed in the case of Al-5 %Si with Al-12 %Si FSW joint. The higher speeds resulted in poor heat generation and plastic flow of the material, which might have resulted in a weak interface at the joint. The higher the welding speeds, the lower the heat produced, which speeded up the cooling of the welded seams. It can also be inferred that when welding rates were higher, there was a lower metallurgical transformation and higher strengths. In the case of Al-5 %Si with Al-12 %Si FSW joint, the tensile strength initially increased with speed but later started reducing.

3.2 Rockwell hardness

The average hardness values obtained for Al-5 %Si with Al-12 %Si and Al-12 %Si with Al-17 %Si FSW joints after the experimentation are given in Table 2. These hardness results are compared for the two dissimilar FSW joints welded at different tool rotational speeds. At a tool rotational speed of 1000 rpm, the hardness increased in both the Al-Si variants. However, the Al-12 %Si with Al-17 %Si dissimilar joint contained a higher percentage of silicon, which led to exceptional hardness and strength.

Table 2: Hardness of FSW joints.

Welding condition	Average Rockwell hardness (RHN)	
	Al-5%Si with Al-12%Si	Al-12%Si with Al-17%Si
710 rpm at 63 mm/min	67.5	62
1000 rpm at 63 mm/min	70.72	78.5
1400 rpm at 63 mm/min	60.5	63.5

3.3 Surface roughness

The results indicated that surface roughness depends on the tool rotational speed and the hardness of the material. Concerning Al-5 %Si with Al-12 %Si FSW joint, it was observed that the surface roughness initially decreased but then increased with the increase in the tool rotational speed. However, in the case of Al-12 %Si with Al-17 %Si FSW joint, the surface roughness decreased with the increase in the tool rotational speed. Table 3 shows the average values obtained for the surface roughness test. The test results with standard deviation bars are represented in Figure 6.

Table 3: Surface roughness values of the FSW joints.

Welding condition	Surface Roughness, Ra (μm)	
	Al-5%Si with Al-12%Si	Al-12%Si with Al-17%Si
710 rpm at 63 mm/min	5.946	4.683
1000 rpm at 63 mm/min	4.404	5.540
1400 rpm at 63 mm/min	7.276	2.870

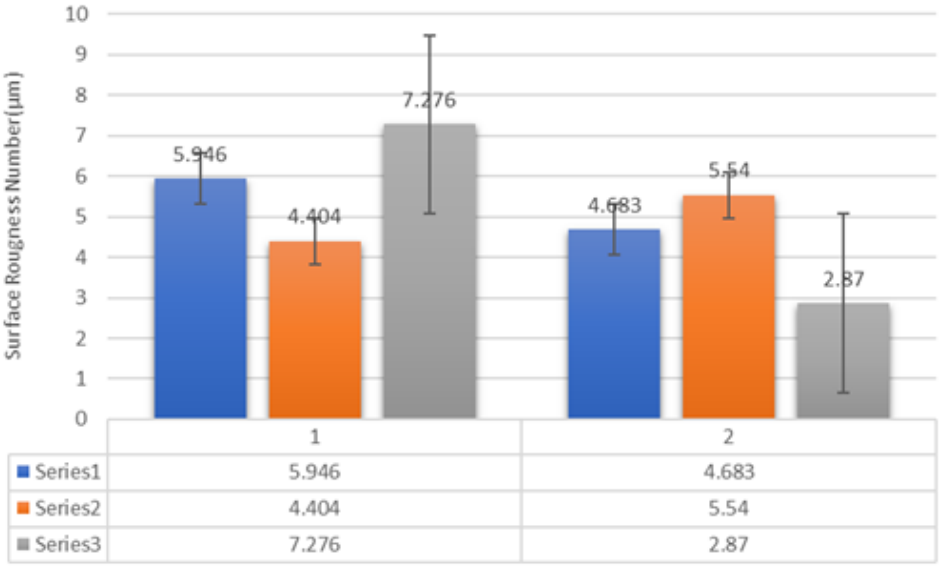

Figure 6: Surface roughness of FSW joints: Series 1 - 710 rpm at 63 mm/min; Series 2 - 1000 rpm at 63 mm/min; Series 3 - 1400 rpm at 63 mm/min.

3.4 Microstructure analysis

A microstructure study was done using Scanning Electron Microscope (SEM) on the weld joints of the friction stir welded specimens. The SEM images were magnified to 200 microns, concentrating on 5 different points (locations) of the weld joints: top, bottom, right, left and the middle region (nugget region). During welding, the plunging force required to drill the Al-5 %Si -Al-12 %Si FSW joint was 12 KN, and for Al-12 %Si -Al-17 %Si FSW joint was more than 20KN. Figure 7, Figure 8 and Figure 9 represent the SEM images for Al-5 %Si -Al-12 %Si FSW joint, while Figure 10, Figure 11 and Figure 12 Al-12 %Si -Al-17 %Si FSW joint.

Figure 7(a) depicts the dispersion of Si particles over the weld joint, where Si needle-like formations can be seen. As seen in the figure, the dynamic recrystallization of this welded connection was minimal. As friction stir welding commences, the tooltip drilled and penetrated the plate stirs the region, as shown in Figure 7(b). As a result of the fact that only a small area is churned in this place, the silicon particles are spread more uniformly. As depicted in Figure 7(c), fewer silicon particles are intermixed on the left side of the weld, which contains 5 % silicon and 95 % aluminum. Consequently, there are fewer silicon particles visible in this view. Due to the low tool rotational speed, it becomes hard to combine the silicon particles. Since it is a known fact that low tool rotating speeds produce lower frictional temperatures, this leads to less mixing of silicon particles during welding. As shown in Figure 7(d), the right side of the weld part is comprised of a 12 % silicon plate, representing a higher silicon content than the region on the advancing side. Therefore, the resultant image contains a large proportion of silicon. The region in Figure 7(e) illustrates that the welding speed is relatively sluggish for perfectly blending silicon particles compared to the other two weld speeds. Evident in this section are features resembling needles.

Figure 8(a) shows the dispersion of silicon particles in fine grains. A few silicon particles have been burned and can be seen as flakes. There are no needle-like structures or cluster formations, which contribute to the absence of crack propagation or defects. The structure in Figure 8(b) differs from that in the top region. Silicon particles form needle-like structures that exist. These needles could be the cause of crack initiation and propagation. When the bottom region is compared to the top region, it is clear that the stirring operation in this area was insufficient. Figure 8(c) shows that the retreating side of the weld zone has fewer silicon particles and needle-like structures. This indicates that a percentage of the silicon was moved from the upper to the lower region during welding. There are also flaws in this area. Figure 8(d) shows tiny silicon grains, indicating that the area was well-welded. It also shows that this region's percentage of silicon particles is lower than in the other. The silicon percentage is the same as in the top region. Figure 8(e) shows similar results to the top and advancing side portions. It is clear that the percentage of silicon is lower. Fine grain-like structures can be seen, indicating a good weld joint in the area.

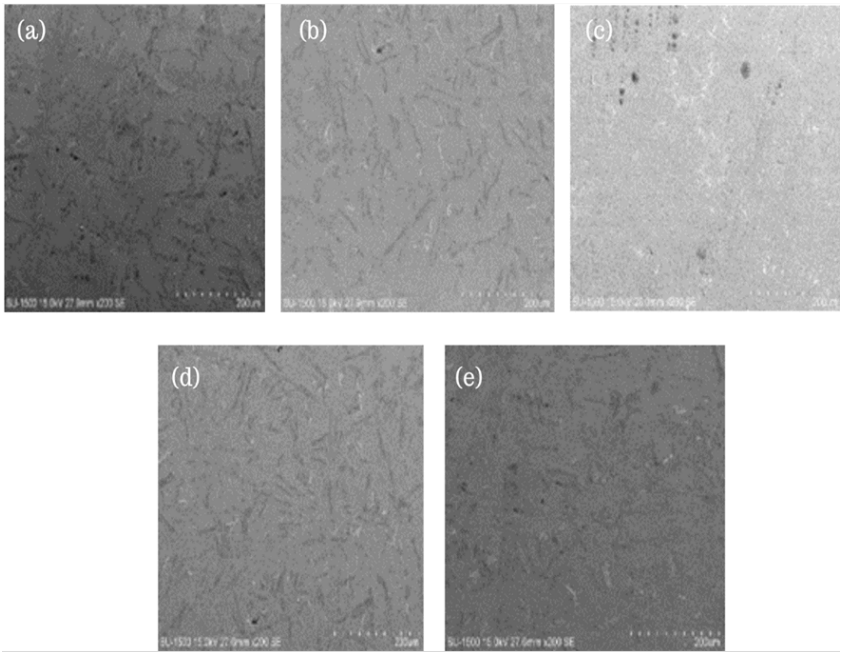

Figure 7: SEM images of Al-5 %Si -Al-12 %Si FSW joint welded using 710 rpm speed at various locations of cross-section: **(a)** top; **(b)** bottom **(c)** Retreating side (left); **(d)** Advancing side (right); **(e)** Nugget zone (middle) portion.

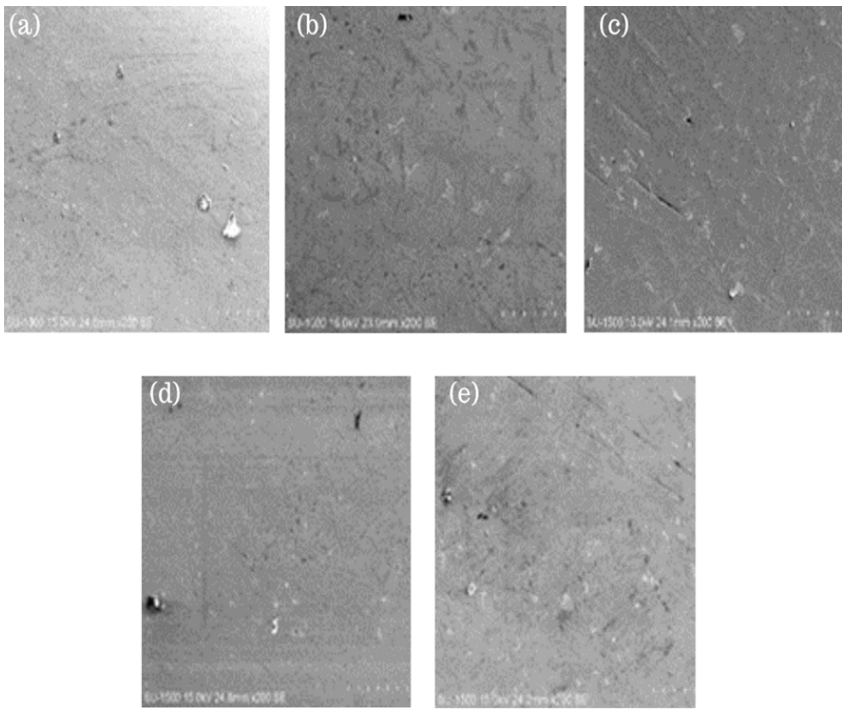

Figure 8: SEM images of Al-5 %Si -Al-12 %Si FSW joint welded using 1000 rpm speed at various locations of cross-section: **(a)** top; **(b)** bottom **(c)** Retreating side (left); **(d)** Advancing side (right); **(e)** Nugget zone (middle) portion.

Figure 9(a) depicts the cross section's top region. The grains in this area have a high silicon content and form tiny, needle-like structures. This is due to the high rotational speed of the tool. Figure 9(b) shows needle-like structures of silicon particles, similar to the weld joint's upper section. This indicates that the particles are properly mixed during welding. Figure 9(c), the retreating side, depicts needle-like structures of silicon particles. It also has a higher percentage of silicon particles. Because of the faster tool rotational speed, silicon can be seen moving from the upper to lower region. However, the region's grain structure is not refined. Silicon is abundant in small grain particles in the region depicted in Figure 9(d). Compared to the other regions of the welded joint, the silicon in this region has been refined. The tool's stirring action in this region improves the distribution of silicon particles. Figure 9(e) depicts the region where silicon can be found in fine grains and needle-like formations. Also visible is the diffusion of silicon particles, similar to that seen in other regions except for the advancing side of the welded region.

Figure 10(a) shows that the welded zone has undergone greater plastic deformation, dispersing the silicon particles into smaller grains. It has gone through less dynamic recrystallization. It also shows that the area has a sound weld from welding. Figure 10(b) shows that silicon particles are present throughout the region as needle structures.

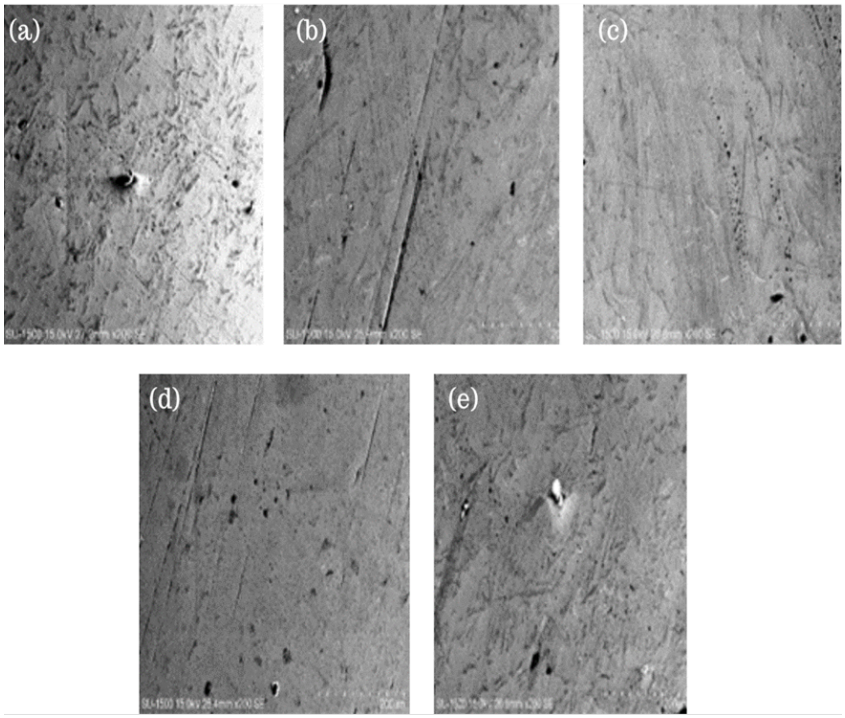

Figure 9: SEM images of Al-5 %Si -Al-12 %Si FSW joint welded using 1400 rpm speed at various locations of cross-section: **(a)** top; **(b)** bottom **(c)** Retreating side (left); **(d)** Advancing side (right); **(e)** Nugget zone (middle) portion.

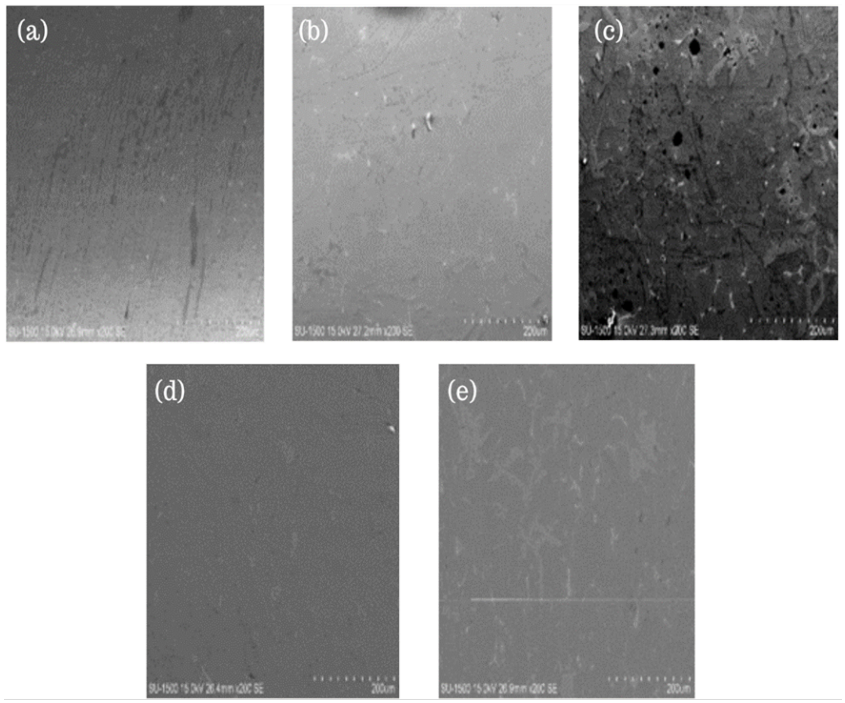

Figure 10: SEM images of Al-12 %Si -Al-17 %Si FSW joint welded using 710 rpm speed at various locations of cross-section: **(a)** top; **(b)** bottom **(c)** Retreating side (left); **(d)** Advancing side (right); **(e)** Nugget zone (middle) portion.

The refinement of the composition did not go well at 710 rpm. Dendrite shapes can also be found in the area. These silicon particles are not distributed evenly throughout the region. Figure 10(c) depicts the formation of clusters of silicon particles throughout the region, as well as the increased hardness and force required to move this silicon due to its higher composition. Defects such as porosity are also visible in the region. The distribution of silicon has not been very good in this region. Figure 10(d) depicts the region containing silicon refined into fine grains. Despite being refined, the silicon is in the form of needle-like structures. Because of the material's higher hardness and a higher silicon percentage, the load required to penetrate this region is high. Figure 10(e) shows that silicon in this region is present in cluster formation due to increased silicon diffusion from the higher region. These cluster formations are more likely to cause crack initiation and propagation. Dendrite shapes can also be found in this region. Most energy has been used to move the silicon from the higher to the lower region.

Compared to the other welded joints, the region shown in Figure 11(a) indicates that most of the silicon has already diffused and is not well refined. However, because silicon diffusion is greater and more evenly distributed, the tensile strength and hardness values obtained at this weld joint are higher than those obtained at the other welded joints. There are also web-like structures in the region. Figure 11(b) shows that silicon is more common and can be found in cluster formation, dendrite formations, and needle-like structures. Fine particles are insignificant in this region. The energy required for material displacement is also higher when compared to the Al-5 %Si with Al-12 %Si FSW joint. Because of the higher percentage of silicon in this region, the hardness and tensile strength are higher. Figure 11(c) shows this region's higher silicon percentage. It can be found in cluster formations but in smaller shapes that are compacted. In this region, the web or dendrite shapes are less visible. Because of the increased hardness, the weld joint has developed a few flaws.

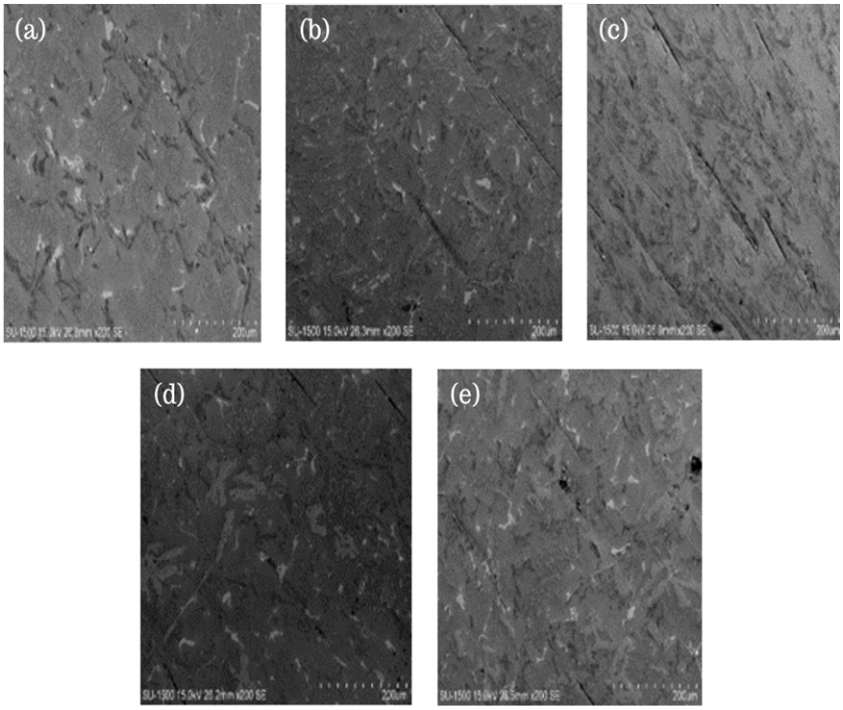

Figure 11: SEM images of Al-12 %Si -Al-17 %Si FSW joint welded using 1000 rpm speed at various locations of cross-section: **(a)** top; **(b)** bottom **(c)** Retreating side (left); **(d)** Advancing side (right); **(e)** Nugget zone (middle) portion.

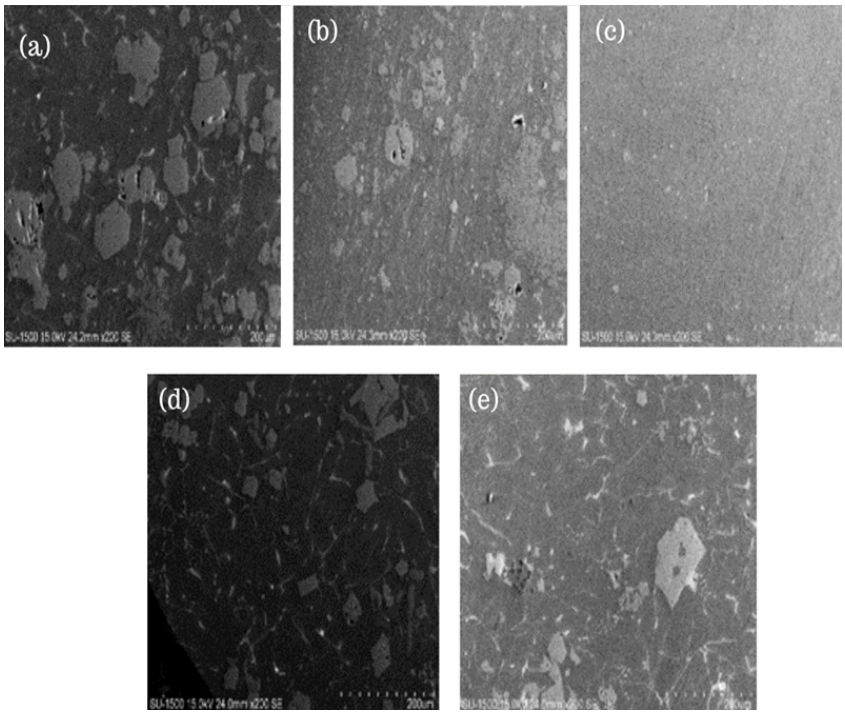

Figure 12: SEM images of Al-12 %Si -Al-17 %Si FSW joint welded using 1400 rpm speed at various locations of cross-section: **(a)** top; **(b)** bottom **(c)** Retreating side (left); **(d)** Advancing side (right); **(e)** Nugget zone (middle) portion.

The presence of silicon in cluster formation and web-like structures indicates that the silicon in the area depicted in Figure 11(d) has not been effectively refined. This region also has a porosity defect. The presence of silicon in cluster formation and web shapes can be seen in the region depicted in Fig. 11(e). There has been no silicon refinement, and its distribution is also not uniform throughout the region. Figure 12(a) shows that silicon is present in cluster and hexagonal shapes. The increased tool rotational speed contributed to less heat generation, resulting in less plastic deformation. The silicon particles have diffused from the higher percentage region to the lower percentage region. The load distribution is also uneven due to the large cluster and hexagonal shapes, resulting in the material failure in the region. Figure 12(b) depicts the presence of silicon in this region in the cluster and hexagonal shapes. However, the silicon is not evenly distributed and is not in the form of fine grains. The composition is completely refined into fine grains in the region depicted in Figure 12(c). However, weld joint diffusion from the higher region is negligible. The material's stirring action only refined the particles in the region, but the displacement of other particles from other regions is not visible. The silicon is present in hexagonal clusters in the area depicted in Figure 12(d). It demonstrates that there is much silicon in the area and that stirring has no effect. The tool rotational speed of 1400 rpm has not been as effective in welding the zone as required for the sound weld. Figure 12(e) shows that silicon diffusion has not been very well in the nugget zone, and the results of hardness and tensile strength indicate a decrease in the same when compared to the welded joint using 1000 rpm speed for Al-12 %Si-Al-17 %Si FSW joint. The silicon distribution in the region is not uniform, making it prone to failure. The variable silicon content of the materials affects most of their mechanical properties. Silicon is diffused from both base materials when they are semi-solid due to heat produced by friction between the surface of the base materials and the tool during welding. By varying the rotational speed of the tool, the variation in the silicon particle distribution can be seen in Figure 12.

4 Conclusion

This research was done to identify the properties of FSW joints made from 6 mm thick plates with Al-Si 5 %, Al-Si 12 %, and Al-Si 17 %. The welding process was carried out at a constant tool feed rate of 63 mm/min. The samples were evaluated for hardness, ultimate tensile strength, surface roughness and microstructure. From the experimental results, it has been observed that Al-12 %Si -Al-17 %Si FSW joints welded using 1000 rpm offered a proper distribution of grains in the weldment, and the same weldment gave well results in hardness number of 78.5 RHN with ultimate tensile strength of 70.12 N/mm^2 for Al-5 %-12 %Si and highest UTS of 78.5 N/mm^2 in Al-12 %Si -Al-17 %Si FSW welded using 1000 rpm. By inspecting the microstructure of the Al-5 %Si -Al-12 %Si FSW joints welded using 1000 rpm; the silicon has been distributed uniformly. Compared to the other two weld joints, this one has less porosity and other defects. At 1400 rpm, the silicon in the Al-12 %Si -Al-17 %Si combination is evenly distributed and has a lower porosity.

Declaration of Competing Interests

The authors declare that they have no known competing financial interests or personal relationships that could have appeared to influence the work reported in this paper.

Funding Declaration

This research did not receive any grants from governmental, private, or nonprofit funding bodies.

Author Contribution

K. J. Santosh Kumar: Conceptualization, Methodology; **Ganesh Arjun Bhargav**: Data curation, Writing- Original draft preparation; **Yuvaraja Naik**: Visualization, Investigation; **K. Bommanna**: Writing- Reviewing and Editing.

References

[1] B. Vijaya Ramnath, C. Elanchezhian, S. Rajesh, S. Jaya Prakash, B. M. Kumaar, and K. Rajeshkannan, "Design and Development of Milling Fixture for Friction Stir Welding," *Materials Today: Proceedings*, vol. 5, no. 1, pp. 1832–1838, 2018.

[2] Q. Chu, W. Y. Li, D. Wu, X. C. Liu, S. J. Hao, Y. F. Zou, X. W. Yang, and A. Vairis, "In-depth understanding of material flow behavior and refinement mechanism during bobbin tool friction stir welding," *International Journal of Machine Tools and Manufacture*, vol. 171, p. 103816, dec 2021.

[3] Z. Y. Ma, A. H. Feng, D. L. Chen, and J. Shen, "Recent Advances in Friction Stir Welding/Processing of Aluminum Alloys: Microstructural Evolution and Mechanical Properties," *Critical Reviews in Solid State and Materials Sciences*, vol. 43, pp. 269–333, jul 2018.

[4] P. L. Threadgill, A. J. Leonard, H. R. Shercliff, and P. J. Withers, "Friction stir welding of aluminium alloys," *International Materials Reviews*, vol. 54, pp. 49–93, mar 2009.

[5] R. P. Singh, S. Dubey, A. Singh, and S. Kumar, "A review paper on friction stir welding process," *Materials Today: Proceedings*, vol. 38, pp. 6–11, 2020.

[6] N. Saini, D. K. Dwivedi, P. K. Jain, and H. Singh, "Surface modification of cast Al-17Engineering, vol. 100, no. January, pp. 1522–1531, 2015.

[7] S. L. Rajaseelan and S. Kumarasamy, "Mechanical properties and microstructural characterization of dissimilar friction stir welded AA5083 and AA6061 aluminium alloys," *Mechanika*, vol. 26, pp. 545–552, dec 2020.

[8] P. Sadeesh, K. M. Venkatesh, V. Rajkumar, P. Avinash, N. Arivazhagan, R. K. Devendranath, and S. Narayanan, "Studies on friction stir welding of aa 2024 and aa 6061 dissimilar metals," *Procedia Engineering*, vol. 75, pp. 145–149, 2014.

[9] M. P. Reddy, A. A. S. William, M. M. Prashanth, S. S. Kumar, K. D. Ramkumar, N. Arivazhagan, and S. Narayanan, "Assessment of Mechanical Properties of AISI 4140 and AISI 316 Dissimilar Weldments," *Procedia Engineering*, vol. 75, no. 2, pp. 29–33, 2014.

[10] M. M. Abd Elnabi, A. B. Elshalakany, M. M. Abdel-Mottaleb, T. A. Osman, and A. El Mokadem, "Influence of friction stir welding parameters on metallurgical and mechanical properties of dissimilar AA5454-AA7075 aluminum alloys," *Journal of Materials Research and Technology*, vol. 8, pp. 1684–1693, apr 2019.

[11] S. Delijaicov, P. A. de Oliveira Silva, H. B. Resende, and M. H. F. Batalha, "Effect of weld parameters on residual stress, hardness and microstructure of dissimilar AA2024-T3 and AA7475-T761 friction stir welded joints," *Materials Research*, vol. 21, aug 2018.

[12] M. Sindhuja, S. Neelakrishnan, and B. S. Davidson, "Effect of Welding Parameters on Mechanical Properties of Friction Stir Welding of Dissimilar Metals- A Review," *IOP Conference Series: Materials Science and Engineering*, vol. 1185, p. 012019, sep 2021.

[13] I. Kalemba-Rec, M. Kopyściański, D. Miara, and K. Krasnowski, "Effect of process parameters on mechanical properties of friction stir welded dissimilar 7075-T651 and 5083-H111 aluminum alloys," *International Journal of Advanced Manufacturing Technology*, vol. 97, pp. 2767–2779, jul 2018.

[14] V. Saravanan, S. Rajakumar, and A. Muruganandam, "Influence of Tool Rotation Speed on Macrostructure, Microstructure and Mechanical behaviour of Dissimilar Friction Stir Welded AA2014-T6 and AA7075-T6 Aluminum Alloys," *Journal of Advances in Mechanical Engineering and Science*, vol. 2, pp. 19–24, aug 2016.

[15] R. Mishra and Z. Ma, "Friction stir welding and processing," *Materials Science and Engineering: R: Reports*, vol. 50, pp. 1–78, aug 2005.

[16] T. Minton and D. J. Mynors, "Utilisation of engineering workshop equipment for friction stir welding," *Journal of Materials Processing Technology*, vol. 177, pp. 336–339, jul 2006.

[17] K. Krishnan, "On the formation of onion rings in friction stir welds," *Materials Science and Engineering: A*, vol. 327, pp. 246–251, apr 2002.

[18] L. Ceschini, I. Boromei, G. Minak, A. Morri, and F. Tarterini, "Effect of friction stir welding on microstructure, tensile and fatigue properties of the AA7005/10 vol.Technology, vol. 67, pp. 605–615, mar 2007.

[19] R. Bhat, N. Mohan, S. Sharma, and S. Rao, "Influence of Seawater Absorption on the Hardness of Glass Fiber/Polyester Composite," *Journal of Computers, Mechanical and Management*, vol. 1, pp. 1–11, oct 2022.

[20] R. K. Bhushan and D. Sharma, "Investigation of mechanical properties and surface roughness of friction stir welded AA6061-T651," *International Journal of Mechanical and Materials Engineering*, vol. 15, p. 7, dec 2020.